STEM CELLS AND DEVELOPMENT
Volume 21, Number 10, 2012

DOI: 10.1089/scd.2011.0390

Intrinsic Growth Deficiencies of Mesenchymal Stromal Cells in Myelodysplastic Syndromes

Carmen Mariana Aanei,[1,2,*] Pascale Flandrin,[1,3] Florin Zugun Eloae,[2] Eugen Carasevici,[2] Denis Guyotat,[3,4] Eric Wattel,[5] and Lydia Campos[1,3]

Myelodysplastic syndromes (MDSs) are clonal disorders of hematopoietic stem cells (HSCs) characterized by ineffective hematopoiesis. MDSs are responsible for 1 or several peripheral cytopenias. The evidence accumulated in recent years demonstrates that in addition to HSC defects, a particular role is also played by stromal microenvironment dysfunctions, which mediate the direct contact with hematopoietic precursor cells (HPCs). These interactions help regulate different adhesion-related processes, such as progenitor cell proliferation, apoptosis, clonogenic growth, and maintenance in in vitro cultures. As previously reported, these interactions are responsible for altering the microenvironment in MDS. Herein, we present a novel selection protocol for obtaining a standards-compliant mesenchymal stromal cell (MSC) preparation. This method allowed us to comparatively analyze 2 subpopulations of bone marrow MSCs (BM-MSCs) in terms of their adhesion profiles and growth abilities: BM-MSCs selected from MDS settings and their normal counterparts. Functional assays revealed that the MSCs from MDS are intrinsically pathological, thus showing a continuous decline of proliferation and a reduced clonogenic capacity during 14 days of culture and in the absence of signals from hematopoietic cells. The MSC growth defects were significantly correlated with decreases in CD44 adhesion molecules and CD49e (α5-integrin).

Introduction

Myelodysplastic syndrome (MDS) disorders result from the gradual expansion of abnormal hematopoietic stem cells (HSCs) associated with the variable suppression of normal hematopoiesis [1]. There is evidence that hematopoietic precursor cells (HPCs) that are isolated from patients with MDS display defective growth in vitro [1,2]. Although numerous studies have addressed the quantitative and qualitative imbalances in cytokine and chemokine levels within the MDS microenvironment [3– 6], there is also convincing evidence that alterations of the direct interaction between HPCs and stroma contribute to abnormal HPC growth and maturation [7–10]. Recent evidence has implicated adhesion protein CD44 in the homing and adhesion of HPCs to mesenchymal stromal cells (MSCs) by the CD44v7 isoform and by the CD44v10 ligand (CD44v10L) that they express [8,11]. In addition, Gottschling et al. showed that β_1-integrins play an essential role in regulating self-renewing HPC divisions within the stromal environment and in maintaining stemness within the first 72 h of homing [10].

In light of these findings, we were interested in evaluating the putative growth deficiencies of MSCs from diseased individuals compared with normal individuals, and we wanted to explore their adhesion profile to identify correlations between these molecules and the MSCs internal capacities for proliferation and functional maturation.

Therefore, we used an immunomagnetic method to select different subpopulations of MSCs and use their phenotypic and functional evaluations.

Numerous attempts have been made to develop more specific procedures for isolation and characterization as well as to establish the hierarchy of different MSC subpopulations. The most common isolation methods are based on MSCs' ability to adhere to plastic or on the use of MSCs' surface epitopes, such as specific markers or adhesion molecules.

Although stromal precursor antigen-1 (STRO-1) is widely regarded as a marker of early mesenchymal stromal precursor cells, it is also expressed on the surface of other human bone marrow (BM) cells that include glycophorin-A^+ nucleated red cells and a small subset of $CD19^+$ B-cells;

[1]Laboratoire d'Hématologie, Hôpital Nord, CHU de Saint-Etienne, Saint-Etienne Cedex, France.
[2]Department of Immunology, Faculty of Medicine, Gr. T. Popa University of Medicine and Pharmacy, Iasi, Romania.
[3]Laboratoire de Biologie Moléculaire de la Cellule, UMR 5239 CNRS, Université de Saint-Étienne, Saint-Étienne, France.
[4]Service Hématologie Clinique, Institut de Cancérologie de la Loire, Saint-Priest-en-Jarez, France.
[5]Oncovirologie et Biothérapies, Centre Léon Bérard, UMR 5239 CNRS, Université de Lyon, Lyon, France.
*Current affiliation: Etablissement Français du Sang Bourgogne–Franche Comté site de Nevers, Nevers, France.

however, it is not expressed in HSCs [12]. This has raised many questions about its use as a specific marker in MSC sorting protocols [13,14]. Plasma membrane-bound ecto-5′-5′nucleotidase (CD73) has been proposed as the most useful molecule for developing robust in vitro MSC assays [14]. However, Simmons et al. reported that the STRO-1^+/glycophorin A^- population has a substantial clonogenic capacity (~100-fold, enriched in colony-forming unit-fibroblast [CFU-F]), which is capable of generating adherent cell layers containing multiple cell types, including adipocytes, smooth muscle cells, and fibroblastic elements; further, this population displays a greater ability to maintain the normal development of the human myeloid lineage than the stromal cells that are commonly isolated from unmanipulated BMs [12]. More recently, Gronthos et al. provided evidence that osteogenic precursors are present in the STRO-1^+ fraction of human BM cells [15]. Psaltis et al. also found a strong correlation between the amount of STRO-1 with mRNA expression of transcription factors related to cellular proliferation and differentiation, which have been associated with an immature, stem-like phenotype [16]. CD73 expression has also been observed in different cells, and its physiological role is to metabolize adenosine 5′-monophosphate to adenosine [17]. CD73 acts as a signal transducing molecule in the human immune system (specifically, it acts as a costimulatory molecule in T cell activation), and it has been shown to be involved in controlling lymphocyte-endothelial cells interactions [18]. It has been hypothesized that CD73 expression in both tumor and host cells protects the tumor from incoming antitumor T cells and suppresses T cell functions through the CD39 (ecto-ATPase)-CD73 axis [19]. Much less is known about CD73 role in MSC biology, but its impact on cell-matrix interactions in chicken fibroblasts has been described [20]. Despite all efforts, there is no common opinion about the expression of these markers on different MSC preparations; reviewing the literature, it is not possible to establish a MSC hierarchy based on STRO-1 and CD73 expression. In this study, we used double selection based on the expression of these markers to isolate MSC subsets from the culture system.

To the best of our knowledge, this is the first study that evaluates the growth patterns of STRO-1^+ and $CD73^+$ MSC fractions derived from patients with MDS compared with normal cells and performs correlations between their adhesion profiles and their growth dysfunctions.

Materials and Methods

Patients

BM aspirates were collected from 8 healthy donors (median age, 63 years) and 20 untreated patients (median age, 73 years), 10 of whom had refractory cytopenia (RC; refractory cytopenia with unilineage dysplasia, and refractory cytopenia with multilineage dysplasia) and 10 of whom had refractory anemia with excess blasts [RAEB; refractory anemia with excess blasts-1 (RAEB-1), and refractory anemia with excess blasts-2 (RAEB-2)]. The patients' assignment to different groups was made according to the 2008 World Health Organization (WHO) classification [21].

Signed, institutional review board-approved, written, informed consent was obtained from all patients and healthy donors.

Amplification of BM-MSCs in cultures

BM mononuclear cells were separated from heparinized BM specimens using density gradient centrifugation. The cells (2×10^6) were seeded in 25-cm^2 culture flasks and expanded to 70%–80% confluence for 4–5 weeks at 37°C with 5% CO_2 in MesenCult® complete medium (StemCell Technologies). The MSCs were allowed to adhere overnight, and nonadherent cells were washed out by changing the medium. Thereafter, the medium was changed twice weekly and replaced with half new medium and half supernatant removed by culture. The MSC layer composition at 80% confluence was evaluated under an inverted microscope after Giemsa staining.

Immunofluorescent evaluation of the normal BM-MSC subpopulations

The cells were thoroughly washed to remove residual media and were fixed in paraformaldehyde 4% w/v for 10 min at room temperature. Fixation was stopped by washing the cells thrice in phosphate-buffered saline (pH 7.2).

Nonspecific background staining was blocked with an antibody (Ab) buffer containing PBS (1×)/fetal calf serum (FCS) (1% w/v)/bovine serum albumin (Sigma-Aldrich; 0.1% w/v) for 1 h. The cells were then permeabilized with 0.1% Triton X-100 (Sigma-Aldrich) in PBS for 20 min before Ab application. Before application, the antibodies were diluted in an Ab buffer of fluorescein isothiocyanate (FITC)-conjugated mouse Anti-Human STRO-1 monoclonal Ab (mAb) (final dilution 1:50, clone sc-47733, Santa Cruz Biotechnology, Inc.) and phycoerythrin (PE)-conjugated mouse Anti-Human CD73 mAb (1:25, clone AD2; BD Pharmingen™). Before acquisition, nuclear staining with 4′,6-diamidino-2-phenylindole (DAPI; 1 μg/mL) was performed for 30 min at 4°C. Slides were mounted in Faramount Aqueous Mounting Medium (Dako Denmark). Double-stained preparations were visualized under an Axio Observer Z1 microscope (Carl Zeiss, Inc.) at 100× magnification with a 0.55 numerical aperture lens. Signals were recorded simultaneously with 3 photomultiplier tubes (PMT 1–3). The images (TIFF format) were captured with a PixeLINK PL-A622C/622000227 camera (Aegis Electronic Group, Inc.) by taking multiple exposures through bandpass optical filter sets appropriate for FITC, Texas Red, and DAPI and using a 100× Plan Apochromat objective.

Immunophenotyping of BM-MSCs with flow cytometry

The MSCs were cultured for 30–35 days. They were then harvested using the MesenCult® Dissociation Kit (StemCell Technologies), collected in glass tubes containing 5 mL MesenCult® with 20% FCS (GIBCO® Invitrogen), and filtered through a 70-μm cell strainer (Falcon, Becton Dickinson). The cell number and viability were evaluated using trypan blue solution (0.4% PBS). The cells were then suspended in 50 μL of washing buffer (PBS containing 1% FCS, and 0.05% EDTA) and stained on ice for 30 min with the following markers: MSC-specific markers (STRO-1, CD73, previously described), endothelium-related markers (Alexa Fluor® 488-conjugated mouse Anti-Human CD31 mAb, clone M89D3, BD Pharmingen; FITC-conjugated mouse Anti-Human CD106 mAb, clone

51-10C9, and BD Pharmingen), adhesion markers (PE-Cy™5-conjugated mouse Anti-Human CD29 mAb, clone MAR4, BD Pharmingen; allophycocyanin (APC)-conjugated mouse Anti-Human CD54 mAb, clone HA58, BD Pharmingen; PE-conjugated mouse Anti-Human CD44 mAb, clone 515, BD Pharmingen; and PE-conjugated mouse Anti-Human CD49e mAb, clone IIA1, BD Pharmingen), and markers associated with hematopoietic lineages (PerCP-conjugated mouse Anti-Human CD45 mAb, clone 2D1, BD Pharmingen; PE-Cy™7-conjugated mouse Anti-Human CD16 mAb, cloneB73.1, BD Pharmingen). Cell viability was evaluated by staining with 1 μL of propidium iodide (PI, 1 mg/mL; Sigma) before FACS acquisition. Data were acquired using an FACS Canto I cytometer and analyzed using DIVA software (Becton Dickinson).

The analysis strategy involved gating for singlet, followed by the exclusion of dead PI^+ cells and final gating using specific marker expression. The level of expression of different markers was normalized using the corresponding median fluorescence intensity ratio (MFIR) for statistical analysis. The adhesion markers were tested at 20 days of culture for 5 different experiments per subpopulation and per study group.

In this study, we determined negative expression for a marker when the MFIR was <2, low- or medium-positive expression when the MFIR was between 2 and 10, and intensely positive expression when the MFIR was >10.

EasySep immunomagnetic selection of STRO-1$^+$ and CD73$^+$ BM-MSCs

To confirm that differences in STRO-1 and CD73 marker expression is the imprint of distinct cell subpopulations, we performed immunomagnetic positive sorting using these markers. The fraction of STRO-1^+ cells was immunodepleted for CD73 by exploiting the differences in epitope density and the avidity of STRO-1 mAb, the STRO-1^+CD73$^-$ cells bearing a higher number of epitope sites (Fig. 3A).

Thus, MSCs, detached as previously described, were stained with Anti-Human CD32 (Fcγ RII) blocker from an EasySep® PE Selection Kit (StemCell Technologies), then with FITC-conjugated mouse Anti-Human STRO-1, 3.0 μg/mL for 10^7 cells for 1 h on ice. Labeled cells were processed by adding EasySep PE Selection Cocktail 100 μg/mL of cells and EasySep Magnetic Nanoparticles and by using the EasySep magnet from the EasySep PE Selection Kit (StemCell Technologies). After the isolation of the STRO-1 positive fraction, the remaining cells were stained with PE-conjugated mouse Anti-Human CD73 mAb (BD Pharmingen), 3.0 μg/mL for 10^7 cells, kept for 1 h on ice, then passed through all the remaining steps (previously described) to select the CD73-positive population. All steps were monitored for purity and viability using flow cytometry.

The STRO-1^+ and CD73$^+$ fractions were enriched to $>95\%$ (96.34 ± 2.26 for STRO-1^+ and 97.74 ± 0.95 for CD73$^+$ cells), and percentages were evaluated from the singlet gate after excluding dead PI^+ cells. Four rounds of selection were performed for each population sorted.

Cell yield and growth characteristics

To assess the growth characteristics of the 2 major MSCs subpopulations, STRO-1^+CD73$^-$ and STRO-1^-CD73$^+$, proliferation and clonogenicity tests were performed. To do so, 1×10^3 viable MSCs (quantified using the trypan blue exclusion test) were plated in 25-cm^2 flasks, and the number of cells was counted on days 1, 7, and 14. We then calculated the proliferation index (the difference between the number of harvested cells and the initial plated number) and the doubling time (the duration of 1 mitosis) estimated by the ratio of the time necessary for 1×10^3 MSCs to reach 80% confluence and the number of population doublings. The number of population doublings was obtained using the following formula: $n = \log(x/y)/\log 2$, where "x" is the number of initial seeded MSCs and "y" is the cell harvest number [22,23].

The clonogenic potential of MSCs was established with plating efficiency (PE) or CFU efficiency assays. After 14 days of culture, the medium was removed, and the colonies were fixed in methanol and treated with Giemsa stain. The colony numbers were then scored. A colony was defined as consisting of at least 50 cells. PE was the ratio of the number of colonies formed to the number of cells seeded $\times 100\%$ [24].

Statistical analysis

Results are expressed as the mean ± standard deviation. The significance level ($P \leq 0.05$) was determined using paired student's t-tests. The SPSS software package (Version 13.0; SPSS, Inc.; www.spss.com) was used for the statistical analysis.

Results

The experiments were configured to isolate and characterize different subsets of MSCs on the basis of STRO-1/CD73 expression, identify the fractions that highlight phenotypic and functional differences in MDS compared with normal cells.

Morphological and morphometric characterization of BM-MSCs from primary cultures in normal and MDS settings

Our study began with the evaluation of MSCs from primary cultures generated from MDS and normal BM aspirates to identify possible structural differences between them.

In line with previous reports, 3 major subpopulations (Fig. 1A) were distinguished in both normal and pathological settings after 30–35 days of culture. The subpopulations were round in shape, with the appearance of undifferentiated cells; thin, spindle-shaped cells; and large, flat cells.

The cellular dimensions and the proportion of different morphological subtypes identified in primary layers of MDS and normal BM cultures are presented in Table 1. The different distribution of the 3 subpopulations of cells in MDS stand out compared with normal settings. However, the slight decrease in the number of large, flat cells in MDS settings, which is considered the onset of terminal differentiation, in addition to the size differences within this population among the different study groups are worth noting. These characteristics could indicate maturation defects.

Three immunophenotypical subpopulations were discriminated from primary BM-MSCs cultures in normal and MDS settings using flow cytometry

In the next step, we decided to further evaluate MSCs amplified in culture for 30–35 days using cytometry and

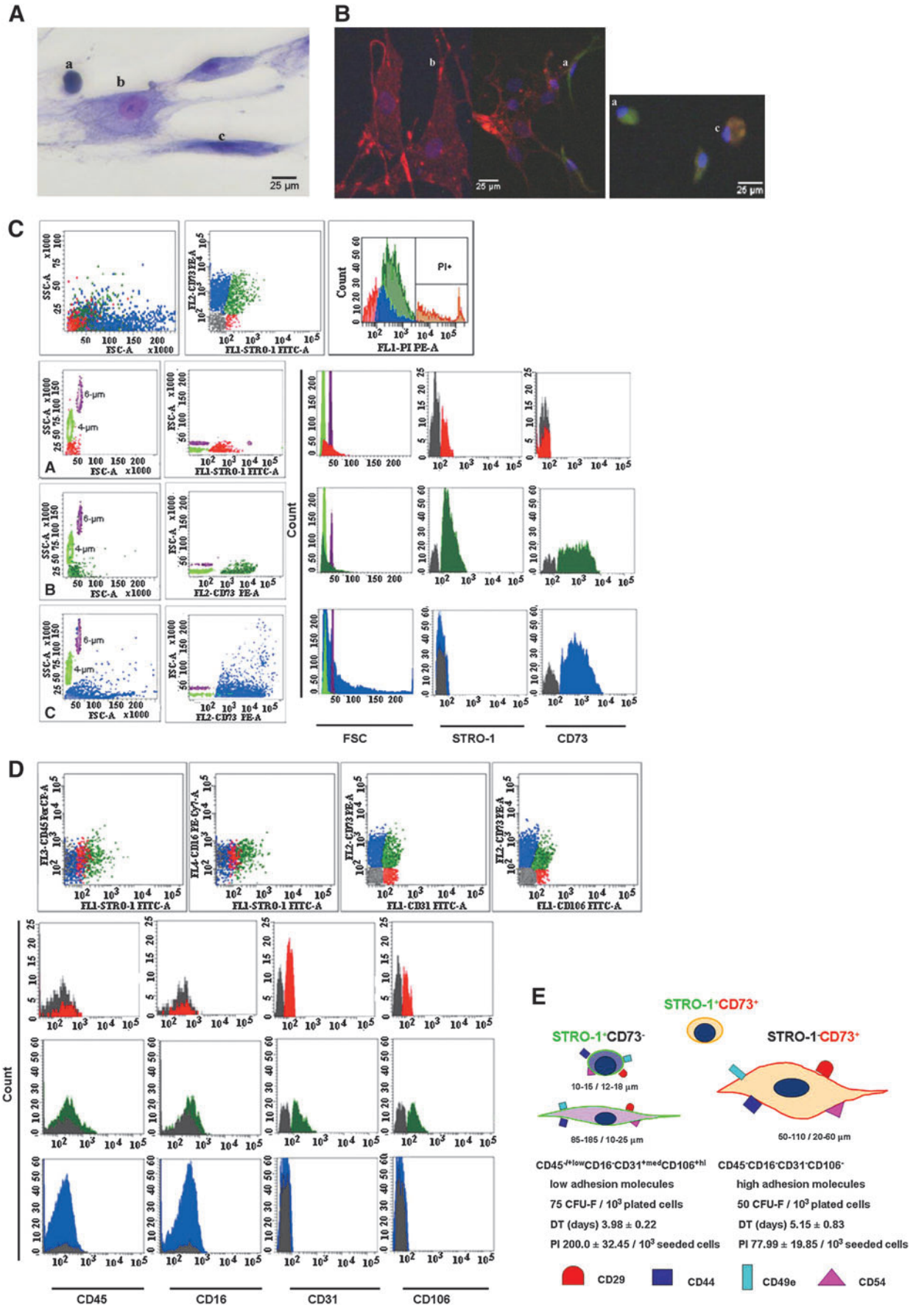
A
a
b
c
25 µm
B
b
a
25 µm
a
c
25 µm
C
SSC-A x1000
FSC-A x1000
FL2-CD73 PE-A
FL1-STRO-1 FITC-A
Count
PI+
FL1-PI PE-A
6-µm
4-µm
A
B
C
FL2-CD73 PE-A
FSC
STRO-1
CD73
D
FL3-CD45 PerCP-A
FL4-CD16 PE-Cy7-A
FL2-CD73 PE-A
FL1-CD31 FITC-A
FL1-CD106 FITC-A
Count
CD45
CD16
CD31
CD106
E
STRO-1+CD73+
STRO-1+CD73-
STRO-1-CD73+
10-15 / 12-18 µm
85-185 / 10-25 µm
50-110 / 20-60 µm
CD45-/+lowCD16-CD31+medCD106+hi
low adhesion molecules
75 CFU-F / 10³ plated cells
DT (days) 3.98 ± 0.22
PI 200.0 ± 32.45 / 10³ seeded cells
CD45-CD16-CD31-CD106-
high adhesion molecules
50 CFU-F / 10³ plated cells
DT (days) 5.15 ± 0.83
PI 77.99 ± 19.85 / 10³ seeded cells
CD29
CD44
CD49e
CD54

Table 1. Mean Dimension and Proportion Among 3 Bone Marrow Stromal Subpopulations After 30–35 Days of Culture in Normal and Myelodysplastic Syndrome Settings

Stroma	*Stromal cell subpopulation*[a]	*Percentages*[b]	*DimensionsH/W (μm)*[c]
NBM	Round-shaped	4.3% ± 1.0%[d]	17.6 ± 5.9/15.0 ± 3.3[d]
	Spindle-shaped	21.7% ± 7.5%[d]	135.2 ± 49.7/18.8 ± 7.5[d]
	Large and flat	**73.9**% ± 8.2%[d]	**83.8 ±** 27.5/38.4 ± 18.0[e]
RC	Round-shaped	8.5% ± 1.2%[d]	15.4 ± 5.6/12.0 ± 4.0[d]
	Spindle-shaped	36.6% ± 2.3%[d]	111.3 ± 15.7/7.6 ± 2.8[d]
	Large and flat	**54.8**% ± 1.0%[d]	**39.2 ±** 38.7/20.4 ± 10.7[e]
RAEB	Round-shaped	16.7% ± 5.4%[d]	16.1 ± 2.1/13.4 ± 2.6[d]
	Spindle-shaped	24.8% ± 11.6%[e]	164.7 ± 96.5/25.4 ± 11.4[e]
	Large and flat	**58.4**% ± 13.2%[e]	**109.1 ±** 50.1/56.5 ± 27.9[e]

[a]Assignment of subtypes was based on morphological characteristics.
[b]Values represent mean percentages from 3 separate experiments ($n = 3$) ± SD from each group of cases.
[c]The mean dimensions were evaluated on $n_{\text{round-shaped}} = 15$, $n_{\text{spindle-shaped}} = 50$, and $n_{\text{large flat}} = 100$ cells from each of the studied groups.
The statistical significance is [d]$P < 0.05$; [e]$P = 0.05$.
NBM, bone marrow-derived stroma from healthy volunteers; RC, stroma derived from refractory cytopenia patients; RAEB, stroma derived from refractory anemia with excess of blasts patients; SD, standard deviation.
The bold values highlight the main differences, in terms of distribution and size, between the three morphological types of stromal cells, in pathological settings compared to normal counterparts.

compare the results with the data obtained from the morphology-morphometry.

In line with the requirements established by the Mesenchymal and Tissue Stem Cell Committee of the International Society for Cellular Therapy [25], our panel of mAbs included specific phenotypical markers in addition to the hematopoietic-related markers CD45 and CD16.

The initial viabilities of the harvested cell fractions, as evaluated by trypan blue exclusion, were 79.6% ± 10.6% for normal stromal cells, 77.6% ± 7.26% for RC stromal cells, and 67.4% ± 10.2% for RAEB stromal cells.

Distinctive features of MSCs (ie, their size and the expression of the specific markers STRO-1 and CD73) allowed us to identify 3 immunophenotypical subpopulations in primary cultures.

In terms of size, cells reading less than 50 on the FSC scale (approximately the size of 4-μm beads) were considered FSC^{low}, those that were ~50 on the FSC scale (the size of 4- to 6-μm beads) were designated FSC^{med}, and those with an FSC greater than 50 (larger 6-μm beads) were designated FSC^{hi} (Fig. 1C). The STRO-1^+ $CD73^-$ population is predominantly FSC^{low} and matched with the smallest population identified in the morphometric analysis. The STRO-1 and CD73 double-positive cells were predominantly FSC^{med}, but the STRO-1^- $CD73^+$ displayed variable FSC values (Fig. 1C). This observation shows that no clear delimitation of cell subsets can be made based on size; supplementary staining with specific markers is required for this purpose. The phenotypic expression of the STRO-1 and CD73 markers associated with cell morphology was then confirmed using fluorescent microscopy (Fig. 1B). The proportions of the 3 cell types at different culture times in normal versus MDS MSC layers, using flow cytometry, are presented in Table 2.

Immunophenotype analysis of the expression of hematopoietic- and endothelium-related markers revealed that in both normal and MDS cells groups, the STRO-1^+ subpopulations STRO-1^+CD73^- and STRO-1^+CD73^+ are $CD45^{+low}$ (MFIR = 2.55 ± 0.78, n = 20, $P < 0.001$), $CD16^-$, $CD31^{+med}$ (MFIR = 8.06 ± 2.87, n = 20, $P < 0.001$), and $CD106^{+hi}$ (MFIR = 12.53 ± 5.32, n = 20, $P < 0.001$). The STRO-1^-CD73^+ subpopulation was negative for all these markers (Fig. 1D). The phenotypic evaluation of MSC layer composition highlights increased percentages of STRO-1^+ cells in 20–30 days of culture that coexpressed CD106 and CD31 in the RAEB and RC groups (Table 2). Moreover, this issue persisted in the MDS groups until 60 days, when cell autolysis occurred.

Comparative analysis of adhesion profiles of BM-MSCs derived from MDS and normal controls

We then studied the adhesion profiles of in vitro amplified MSCs using a combination of mAbs raised against surface adhesion markers, VLA_5 or α-5 β1 integrin (CD49e, CD29), intercellular adhesion molecule 1 or CD54, and the

FIG. 1. Characterization of normal BM-MSCs amplified for 30–35 days in primary cultures. Morphological appearance (Giemsa stain; magnification, ×40): a, small, round, undifferentiated cells; b, large, flat cells; and c, spindle-shaped cells **(A)** and immunofluorescence labeling **(B)**. Human MSCs were double stained for STRO-1 (*green*) and CD73 (*red*). Cell nuclei are 4′,6-diamidino-2-phenylindole-stained (*blue*). Flow cytometry evaluation according to size and expression of STRO-1 and CD73: FSC^{low} STRO-1^{+low} $CD73^-$ (*red*), FSC^{med} STRO-1^+ $CD73^+$ (*green*), and FSC^{var} STRO-1^- $CD73^+$ (*blue*) **(C)**. Two types of reference beads with 4-μm and 6-μm sizes were run parallel to the cells for FSC standardization. Hematopoietic and endothelium-related marker expression **(D)**. Representative histograms were presented for each subtype of cells, as discriminated by STRO-1 and CD73 expression. Marker expression was compared with autofluorescence in unstained cells (*gray*). Summary of morphology, immunophenotype, and growth characteristics of the STRO-1^+ $CD73^-$ and STRO-1^- $CD73^+$ cells **(E)**. PI and DT were evaluated at the time of harvesting (80% confluence; 14 days of culture) for 10^3 seeded cells. BM, bone marrow; DT, doubling time; MSC, mesenchymal stromal cells; PI, proliferation index; STRO-1, stromal precursor antigen-1.

Table 2. Bone Marrow-Mesenchymal Stromal Cell Subpopulations in Normal and Myelodysplastic Syndrome Environments Evaluated Using Flow Cytometry Over the Course of 60 Days of Culture

BM-MSC primary culture	*BM-MSC subpopulation*	*Day 10*	*Day 20*	*Day 30*	*Day 40*	*Day 60*
NBM	STRO-1$^+$CD73$^-$					
	%	5.0±2.5	22.0±9.2	12.9±6.9	16.4±6.7	21.9±3.2
	Cell count	1.0±0.5	4.4±1.8	2.6±1.4	3.3±1.3	4.4±0.6
	STRO-1$^+$CD73$^+$					
	%	17.0±9.9	25.8±6.4	21.7±3.3	24.2±5.9	0.7±0.2
	Cell count	3.4±2.0	5.2±1.3	4.3±0.7	4.8±1.2	0.1±0.01
	STRO-1$^-$CD73$^+$					
	%	78.0±11.6	52.2±9.1	65.4±9	59.4±11.3	77.4±3.4
	Cell count	15.6±2.3	10.4±1.8	13.1±1.8	11.9±2.3	15.5±0.7
RC	STRO-1$^+$CD73$^-$					
	%	7.3±1.5	13.8±5	**19.5**±5.5	10.7±2.8	15.3±4.1
	Cell count	1.5±0.3	2.7±1.0	**3.9**±1.1	2.1±0.6	3.1±0.8
	STRO-1$^+$CD73$^+$					
	%	20.9±2.6	20.4±9.8	**27.6**±5.0	**43.0**±10.2	**39.5**±5.1
	Cell count	4.2±0.5	4.1±2.0	**5.5**±1.0	**8.6**±2.0	**7.9**±1.0
	STRO-1$^-$CD73$^+$					
	%	71.8±7.1	65.8±12.7	52.9±6.6	46.3±7.9	45.2±6.9
	Cell count	14.3±1.4	13.2±2.5	10.6±1.3	9.3±1.6	9.0±1.4
RAEB	STRO-1$^+$CD73$^-$					
	%	6.1±3.3	**64.7**±9.0	**45.4**±9.0	15.0±4.1	6.6±1.4
	Cell count	1.2±0.7	**12.9**±1.8	**9.1**±1.8	3.0±0.8	1.3±0.3
	STRO-1$^+$CD73$^+$					
	%	18.1±1.5	6.8±3.2	14.0±5.8	18.0±4.1	**24.2**±7.1
	Cell count	3.6±0.3	1.4±0.6	2.8±1.2	3.6±0.8	**4.8**±1.4
	STRO-1$^-$CD73$^+$					
	%	75.8±5.7	28.5±7.4	40.6±9.5	67.0±7.0	69.2±13.6
	cell count	15.2±1.1	5.7±1.5	8.1±1.9	13.4±1.4	13.9±2.7

The values are the mean percentage and actual cell count±SD from 8 separate experiments.
Cell count = mean of actual cell count $\times 10^3$.
The significance level is $P < 0.05$.
MSC, mesenchymal stromal cell; STRO-1, stromal precursor antigen-1.
The bold values highlight the main differences, in terms of distribution of the three BM-MSCs subpopulations discriminated by STRO-1 and CD73 expression, in MDS settings vs. normal controls.

Table 3. Summary of the Adhesion Profile for In Vitro Expanded Mesenchymal Stromal Cells from Patients with Normal and Myelodysplastic Syndrome

		CD29		*CD54*		*CD44*		*CD49e*	
		% of CD29$^+$ cells	*MFIR*	*% of CD54$^+$ cells*	*MFIR*	*% of CD44$^+$ cells*	*MFIR*	*% of CD49e$^+$ cells*	*MFIR*
NBM	STRO-1$^+$CD73$^-$	29.4±11.0	45.6±13.4	27.2±9.0	18.3±4.1	34.6±12.6	3.6±1.9	38.0±15.7	4.3±2.6
	STRO-1$^+$CD73$^+$	34.3±46.7	**134.8**±46.7	30.3±32.8	**46.2**±17.7	32.0±16.6	**55.2**±21.7	28.6±4.0	**31.3**±3.7
	STRO-1$^-$CD73$^+$	66.3±14.8	**102.4**±25.9	64.8±12.7	**30.8**±12.4	72.4±16.9	**69.6**±22.9	70.9±11.0	**31.2**±16.9
RC	STRO-1$^+$CD73$^-$	9.9±3.5	44.2±20.2	7.9±3.6	12.1±3.5	18.6±8.8	4.8±2.7	14.0±5.2	6.0±1.6
	STRO-1$^+$CD73$^+$	12.6±5.2	**54.6**±18.1	10.9±4.9	**21.7**±5.3	8.9±1.9	**9.2**±3.9	13.9±8.8	**19.6**±5.9
	STRO-1$^-$CD73$^+$	82.7±7.6	**28.6**±9.0	79.8±9.8	**12.4**±5.6	81.5±17.6	**6.4**±2.6	69.7±7.3	**15.8**±4.7
RAEB	STRO-1$^+$CD73$^-$	59.2±7.7	18.2±4.1	56.2±4.5	22.1±5.2	73.7±15.6	2.5±0.8	71.2±13.7	3.8±1.3
	STRO-1$^+$CD73$^+$	6.6±2.4	**43.2**±14.6	7.1±2.9	**28.7**±10.2	5.6±3.2	**12.5**±1.7	4.9±0.3	**15.4**±2.5
	STRO-1$^-$CD73$^+$	40.3±10.3	**54.5**±18.9	37.6±11.1	**23.0**±5.0	20.7±3.0	**19.1**±5.5	36.6±12.6	**9.6**±5.3

Values represent the median MFIR of adhesion markers±SD from 5 different experiments, evaluated for each subpopulation and group of cases after 20 days of culture.
The statistical significance level was $P < 0.001$.
MFIR, median fluorescence intensity ratio.
The bold values reflect the main differences, in terms of intensity of expression, for the adhesion markers evaluated on BM-MSCs from MDS settings compared to normal counterparts.

extracellular matrix protein CD44. We noticed a homogeneous expression of adhesion markers, regardless of the subpopulation analyzed or the case group (Table 3).

In the $CD73^+$ subsets of cells, which did or did not co-express STRO-1, we noticed a significant reduction in CD54 and CD29 expression (~2- and 3.5-fold in dysplastic cells versus normal cells) when compared with the same subpopulations of cells, but these modifications did not reach statistical significance.

Significant differences were noticed for CD44 and CD49e markers. The CD44 drop was substantial in the STRO-1^- $CD73^+$ (11-fold) and STRO-1^+CD73^+ (6-fold) subpopulations from the RC group and lower in the same groups of cells from the RAEB group (3.5-fold and 4-fold, respectively). Statistical significance was achieved for the differences in CD44 expression in STRO-1^+CD73^+ subpopulations ($P=0.001$ for STRO-$1^+CD73^+_{RC}$ and $P<0.001$ for STRO-$1^+CD73^+_{RAEB}$) compared with normal counterparts. A downward trend for CD49e was also noticed in MDS MSCs in both subpopulations of $CD73^+$, registering 2-fold reductions (Fig. 2). Statistical significance was reached for both subpopulations of cells (STRO-1^+CD73^+ and STRO-1^-CD73^+) regarding CD49e expression in RAEB-derived cells compared with normal counterparts ($P=0.002$ for STRO-$1^+CD73^+_{RAEB}$ and $P<0.001$ for STRO-$1^-CD73^+_{RAEB}$).

Functional properties of the STRO-1^+ $CD73^-$ and STRO-1^- $CD73^+$ MSC subclasses selected from MDS and healthy volunteers

The next steps of the study addressed subpopulations that were determined according to their specific expression of STRO-1 and CD73 markers (Fig. 3A). This selection was performed to allow the functional characterization of different cell fractions and to reduce the errors that result from comparing the different biological systems, regardless of whether the structural differences between the MDS and normal MSC primary layers are taken into account.

In the normal settings, the proliferation tests for STRO-1^+CD73^- and STRO-1^-CD73^+ fractions revealed a plateau phase in the first 7 days of culture and logarithmic growth in the next 7 days. The STRO-1^+CD73^- fractions proliferated more efficiently than the STRO-1^-CD73^+ fraction. The average proliferation index for STRO-1^+CD73^- cells was 200.0 ± 32.45 versus. 77.99 ± 19.85 for STRO-1^-CD73^+ cells at the harvesting

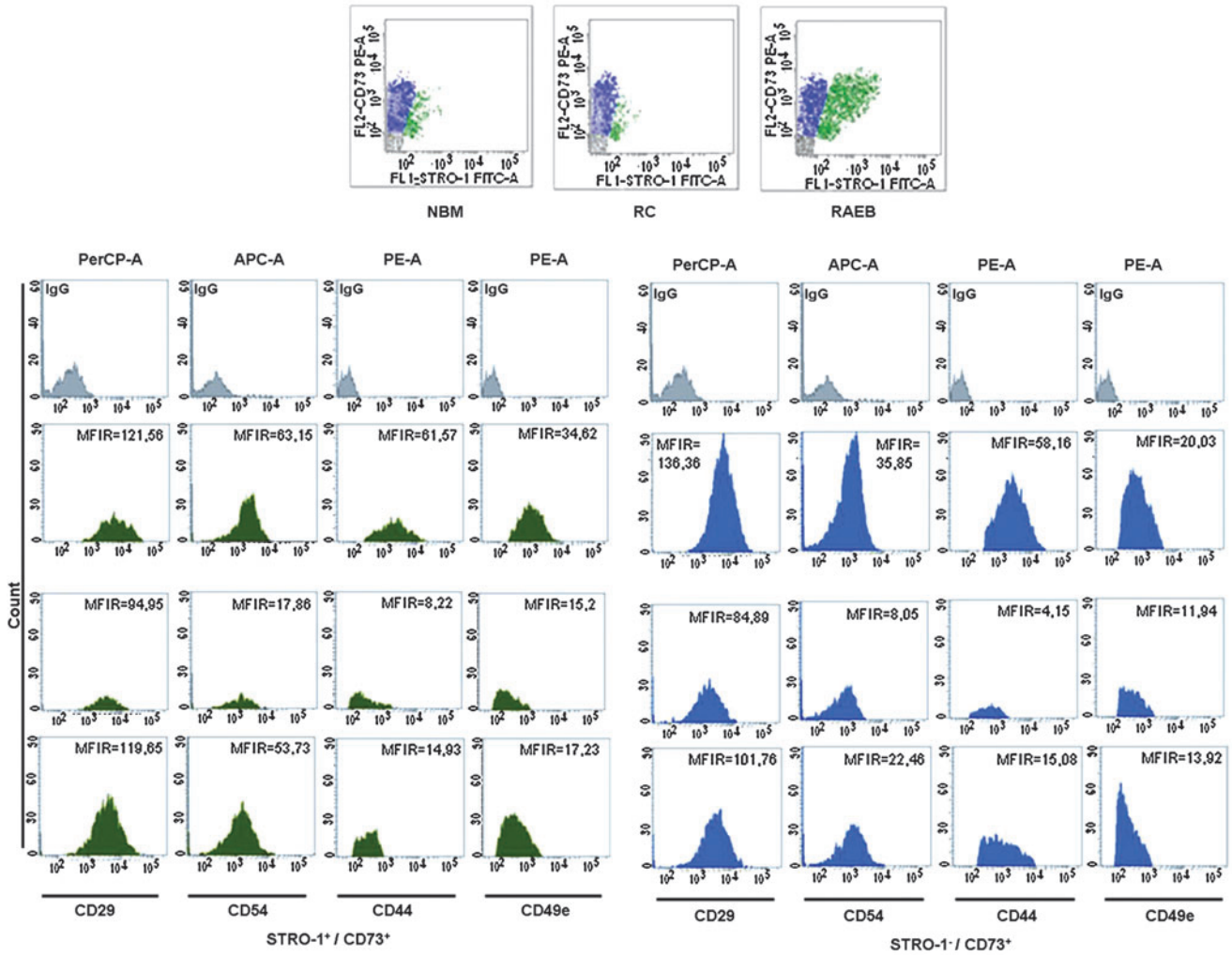

FIG. 2. Pattern of adhesion marker expression on BM-MSCs isolated from patients with MDS compared with that of healthy volunteers. Representative examples of adhesion marker expression on STRO-1^+CD73^+ cells (*green*) and STRO-1^-CD73^+ cells (*blue*) compared with isotype-matched controls (*gray*). MDS, myelodysplastic syndrome.

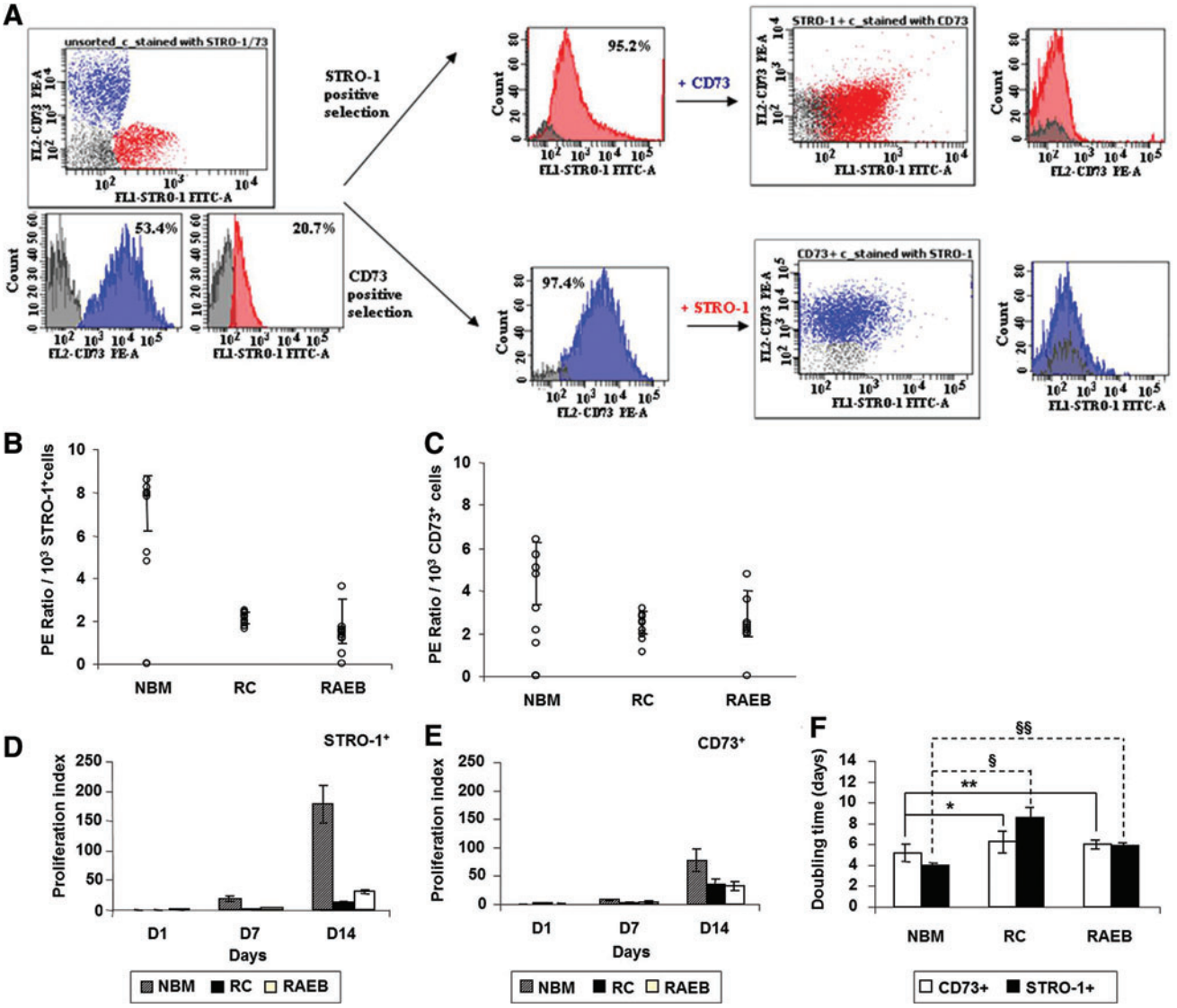

FIG. 3. Experimental strategy of STRO-1/CD73 Immunomagnetic Selection **(A).** Growth kinetics of STRO-1$^+$CD73$^-$ and STRO-1$^-$CD73$^+$ MSC sorted cells from normal and MDS BM **(B–F)**. Plating efficiency of STRO-1$^+$ MSCs **(B)** and CD73$^+$ MSCs **(C)**. Proliferation index **(D, E**; NBM = left column, RC = middle column, and RAEB = right column**)** and cell-doubling time **(F)** of STRO-1$^+$ and CD73$^+$ cell fractions from patients with MDS compared with normal cells. All values reflect the mean ± SD. The results obtained for different groups of cases and for the 2 fractions investigated were significantly different ($P < 0.05$). Comparisons between fractions sorted from patients with MDS versus normal counterparts for 8 experimental groups ($^{\S}DT_{RC\ STRO\text{-}1^+}$ vs. $DT_{NBM\ STRO\text{-}1^+}$; $^{\S\S}DT_{RAEB\ STRO\text{-}1^+}$ vs. $DT_{NBM\ STRO\text{-}1^+}$; $^{*}DT_{RC\ CD73^+}$ vs. $DT_{NBM\ CD73^+}$; $^{**}DT_{RAEB\ CD73^+}$ vs. $DT_{NBM\ CD73^+}$) are presented: $^{*}P = 0.034$; $^{**}P = 0.242$; $^{\S}P = 0.008$; $^{\S\S}P = 0.002$, respectively. Similar viabilities (CV < 5%) were observed for the STRO-1$^-$ and CD73$^-$ selected fractions from the 3 groups (for STRO-1$^+$ fractions: $NBM_{STRO\text{-}1+\ viability=}$ 96.4 ± 2.0, $RC_{STRO\text{-}1+\ viability=}$ 95.5 ± 3.4, and $RAEB_{STRO\text{-}1+\ viability=}$ 95.3 ± 3.6; and for CD73$^+$ fractions: $NBM_{CD73+\ viability=}$ 97.1 ± 1.7, $RC_{CD73+\ viability=}$ 95.3 ± 3.2, $RAEB_{CD73+\ viability=}$ 96.2 ± 3.0). The values represent the mean percentages ± SD of viable cells as evaluated by trypan blue exclusion. RAEB, refractory anemia with excess blasts; RC, refractory cytopenia; SD, standard deviation. Color images available online at www.liebertonline.com/scd

time (Fig. 3D, E), and the plating efficiency of STRO-1$^+$CD73$^-$ cells was 7.5% ± 1.28%, compared with 4.83% ± 1.48% in the STRO-1$^-$CD73$^+$ fraction, for 10^3 seeded cells (Fig. 3B, C).

MSC production in STRO-1$^+$ and CD73$^+$ cell cultures from MDS marrows was deficient (Fig. 3D–F).

The average proliferation indexes of the STRO-1$^+$ fractions from RC and RAEB patients were 17 times and 6.5 times lower than that of the normal controls, respectively (Fig. 3D–F). Moreover, for CD73$^+$ fractions, a 2.5-fold drop was recorded in patients with RC and RAEB compared with normal MSC output (Fig. 3D–F).

In addition, the clonogenic ability of the fractions selected from MDS settings was strongly diminished, and the differences were more obvious for the STRO-1$^+$ CD73$^-$ cells (Table 4).

Thus, the MSCs selected from the RC group showed a clonogenic capacity that was 3.5 times lower for STRO-1$^+$CD73$^-$, and ~2 times lower for STRO-1$^-$CD73$^+$

Table 4. Relative Colony-Forming Unit-Fibroblast Numbers Obtained for STRO-1$^+$ and CD73$^+$ Fractions Selected from Myelodysplastic Syndrome Compared with Normal Settings

		STRO-1$^+$ CD73$^-$ MSCs	*CD73$^+$ STRO-1$^-$ MSCs*
NBM ($n=8$)	% viable cells[a]	96.4 ± 2.0	97.1 ± 1.7
	% purity[b]	98.5 ± 1.2	99.2 ± 0.7
	CFU-F No./10^3 plated cells	74.6 ± 3.4	49.5 ± 10.2
RC ($n=8$)	% viable cells[a]	95.5 ± 3.4	95.3 ± 3.2
	% purity[b]	98.0 ± 0.9	98.9 ± 0.6
	CFU-F No./10^3 plated cells	22.2 ± 3.8	23.9 ± 11.6
RAEB ($n=8$)	% viable cells[a]	95.3 ± 3.6	96.2 ± 3.0
	% purity[b]	98.2 ± 1.3	98.7 ± 1.0
	CFU-F No./10^3 plated cells	19.3 ± 5.9	29.7 ± 9.4

The results are expressed as the mean ± SD from the indicated number of independent experiments.
The significance level is $P < 0.05$.
[a]The percentage of viable cells was evaluated by trypan blue exclusion assay.
[b]The purity of selected fractions was evaluated by flow cytometry, and the values presented are the mean percentage of CD73$^+$ STRO-1$^-$ PI$^-$/STRO-1$^+$ CD73$^-$ PI$^-$ cells with singlet gating.
CFU-F, colony-forming unit-fibroblast; PI, propidium iodide.

compared with normal counterparts. The same decline was noticed for RAEB selected cells compared with normal cells (~4 times lower for STRO-1$^+$CD73$^-$ fractions and 1.65 times lower for STRO-1$^-$CD73$^+$ cells) (Fig. 3B, C).

In conclusion, the relative proliferation of MDS cultures is the result of a division process that is continuous, but occurs at a low rate and without the ability to generate the normal functional progenitors required to form colonies.

Decreased adhesion marker expression negatively correlates with MSC growth in MDS

To evaluate the adhesion abnormalities' significance to the functional integrity of the MSC layers in MDS, the statistical correlations of their functional parameters were determined.

A first observation resulting from this analysis was that despite a decrease in CD54 and CD29 expression in dysplastic MSCs, the comparative statistical analysis did not produce significant correlations.

However, significant correlations were obtained for the other 2 markers, CD44 and CD49e.

As indicated in Fig. 4A, a positive relationship was observed between the reduced intensity of CD44 expression in STRO-1$^+$CD73$^+$ cells in the RC and RAEB groups and the CFU efficiency obtained for CD73$^+$ subsets of cells.

Moreover, the increased level of CD49e expression noticed in STRO-1$^+$CD73$^+$ and STRO-1$^-$CD73$^+$ cells was inversely correlated with the doubling times calculated for STRO-1$^+$ and CD73$^+$ fractions sorted from the same samples from RAEB cases (Fig. 4B).

This evidence supports the theory that MSC expansion is an adhesion-dependent process and that CD44 and CD49e molecules are involved in this process.

Discussion

MSCs are found in many locations, but their main reservoirs are the BM and periosteum [26]. Despite numerous attempts to characterize and understand the biology of these cells, the data remain scarce and controversial. As in previous reports [6,27], we found that isolation methods have a huge impact on the composition of MSC preparations and cause tremendous differences in different groups' results. Further, the phenotypic pitfalls are related to the cells' detachment from the culture [28,29]. In this study, we noticed a reduction in the percentages of positive cells and a decrease in MFIR for the following markers: CD29, CD49e, CD44, CD31, and CD106 by trypsinization (data not shown).

The current study has extended the characterization of MSCs prepared with immunoselection using 2 specific markers, STRO-1 and CD73, by documenting their morphology-morphometry, phenotype, and growth kinetics. Immunomagnetic selection allowed us to isolate 2 major subpopulations. The first subpopulation, STRO-1$^+$ CD73$^-$ cells, is less abundant in normal BM controls and displays a round or spindle shape, and, in terms of size, the cells in this population range from 5 to 26 μm. Phenotypically, they express low levels of CD45, adhesion molecules, and the endothelial-related markers CD31(PECAM-1) and CD106 (VCAM-1). In terms of growth abilities, these cells show a higher proliferation index, and they have clonogenic potential 1.5 times greater than their STRO-1$^-$ CD73$^+$ counterparts. By contrast, the STRO-1$^-$CD73$^+$ fraction includes mostly larger (50 to 110 μm, on average) and more granular cells that are negative for endothelial- and hematopoietic-related markers, but they express increased levels of the adhesion markers CD44, CD54, CD29, and CD49e, which correlates with their lower rate of proliferation ($77.99 \pm 19.85/10^3$ CD73$^+$ seeded cells vs. $200.0 \pm 32.45/10^3$ STRO-1$^+$ seeded cells) (Fig. 1E). This difference in the expression of adhesion markers may reflect the different roles of these cells within their own in vitro niche. Prockop DJ noticed in MSC cultures a population of cells that express surface proteins with an inhibitory influence on cell adhesion [such as α_6-integrin and podocalyxin-like protein (PODXL)]. These cells are highly motile, secrete DKK-1 (an inhibitor of the canonical Wnt signaling pathway), and serve as nurse cells for other subpopulations; thus, they are key elements of the rapid growth phase [30]. Technically, the 2 fractions could be exploited differently, STRO-1$^+$ cells being more robust for carrying out in vitro MSC growth assays, whereas CD73$^+$ cells have proved their utility in the evaluation of adhesion profiles. Moreover, Simmons and Torok-Storb have claimed that a STRO-1$^+$ stroma layer represents a good

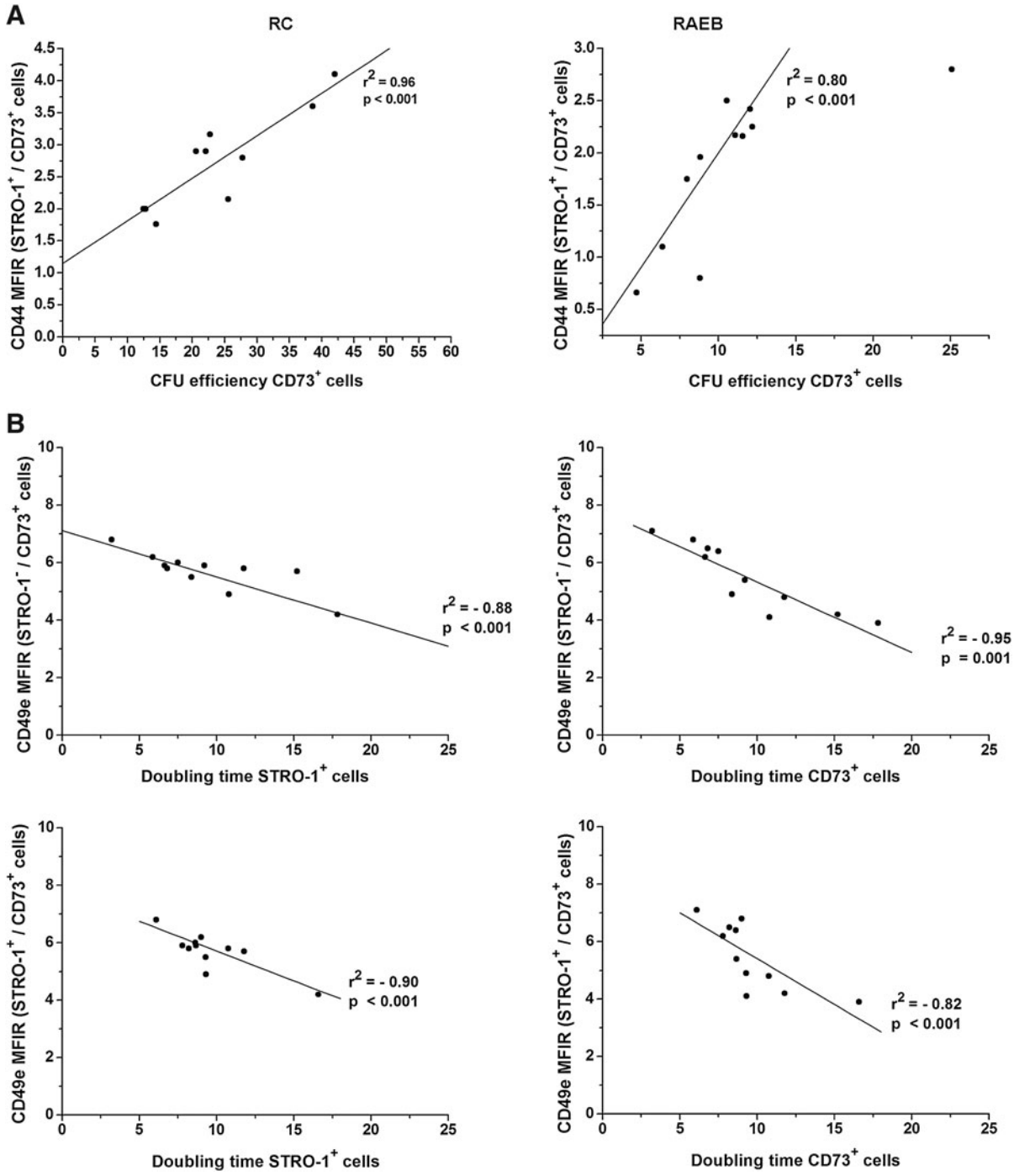

FIG. 4. CD44 and CD49e significance for MSC growth in MDS settings. The plating efficiency of $CD73^+$ cells selected from MDS settings versus the intensity of CD44 expression reflect that their clonogenical potential is directly correlated with CD44 expression. The CFU efficiency of $CD73^+$ cells was calculated for 1×10^3 seeded MSCs **(A)**. CD49e expression in pathological MSCs and its impact on the proliferative potential of STRO-1^+ and $CD73^+$ cells **(B)**. CFU, colony-forming unit.

alternative for an in vivo stroma for performing assays to evaluate HPC-MSC contacts. The STRO-1 molecule does not by itself affect the proliferative abilities of HPCs, and it has low affinity for complement. Thus, the STRO-1 layer appears to only provide signals when induced by the engagement of other adhesion molecules [12].

The CD106 expression was previously reported in umbilical cord blood and BM-derived MSCs [27,31], seems to be the imprint of a particular location (the nearby outer surfaces of blood vessels), and may share an identity with the vascular pericytes [32,33]. This hypothesis is supported by the coexpression of α smooth muscle actin or 3G5 antigen, which is recognized as a specific marker for pericytes [34]. Further evidence is the fact that a minor subpopulation of $STRO^{+hi}$ VCAM-1^+ cells isolated from freshly BM, described as lacking the Ki-67 antigen, appears to be a noncycling population in vivo, exhibits telomerase activity, and shows an undifferentiated phenotype and substantial proliferation in

vitro [34]. Their unlimited potential for division and proliferation is also supported by observations that the small number of STRO-1$^+$ cells seen in cultures at later points were able to produce adherent cell layers with the same cellular composition and phenotype as those generated by STRO$^+$ cells freshly isolated from BM [12].

Under the MDS condition, we noticed a higher number of STRO-1$^+$ cells that coexpressed CD106 and CD31 between 20 and 30 days of culture and which persisted until 60 days.

Two hypotheses can be evoked from the expression of these markers in relation to MDS physiopathology: the first is related to CD106 upregulation induced by TNFα stimulation [31], and the second is related to CD106 function as a major ligand for selective CD29-mediated HPC-to-MSC adhesions, and, thus, its influence on the HPC mitotic rate and division kinetics [10].

Higher TNFα levels are common in MDS [34], and the MSCs themselves could be responsible for its synthesis in the absence of HPC stimulation. The role of this cytokine in the MDS microenvironment is probably related to its capacity to induce internal proliferative signals in MSCs, as previously noted by Kohase et al. [35].

The increased expression of CD31$^+$ could be an imprint of the neoformation of blood vessels in MDS settings, as we showed in a previous study [36].

Further, the functional tests revealed MSC growth abnormalities in the absence of any contact with or stimulation by soluble molecules from HPCs and proved the pathological nature of stromal precursors in MDS settings (Fig. 3). To summarize the biological characteristics of MSCs selected from patients with MDS, 2 different patterns were observed in relation to the type of MDS. For the RC group, similarly reduced clonogenic capacity was observed for both selected fractions, STRO-1$^+$ and CD73$^+$, and a dramatic decrease in proliferation was largely attributable to the STRO-1$^+$ cells. This issue could be explained by an extension of their doubling time to 3-fold that of normal cells (and even 1.3-fold that of RAEB cells) despite their persistence during 60 days of culturing. Similarly, the CD73$^+$ fraction was unable to proliferate and produce colonies, and this reduced CFU-F number directly correlates with the loss of CD44 on their surface (Fig. 4A). By contrast, in RAEB, the proliferation rate is moderately improved due to the reduced doubling time of STRO-1 cells. However, at the end point, this was not accompanied by complete functional maturity as reflected in the CFU-F number. Overall, the doubling time of MSCs was found to inversely correlate with their CD49e expression (Fig. 4B).

In conclusion, in MDS settings, an increased number of STRO-1$^+$ precursors persist with the capacity for continuous division. Since they do so at a low rate and lack the ability to complete asymmetric divisions and produce mature functional progenitors, this phenomenon might reflect the expansion of an abnormal MSC clone over time with concomitant suppression of residual normal stem cells.

Further cytogenetic studies and transcriptome decryption of MDS MSCs are required to evaluate the molecular substrate of these deficiencies.

Acknowledgments

The authors acknowledge the expertise of J. F. Mayol (CRSSA Emile Pardé, 38702 La Tronche, France) in the MSC functional assays and of C. Lambert (Immunology Laboratory, University Hospital St. Etienne, 42055, Saint-Etienne, France) in cell sorting. Funding was provided by "Ligue Départementale contre le Cancer de la Loire," "Association Les Amis de Rémi" (France).

Author Disclosure Statement

No competing financial interests exist.

References

1. Coutinho LH, CG Geary, J Chang, C Harrison and NG Testa. (1990). Functional studies of bone marrow haemopoietic and stromal cells in the myelodysplastic syndrome (MDS). Br J Haematol 75:16–25.
2. Tennant GB, V Walsh, LN Truran, P Edwards, KI Mills and AK Burnett. (2000). Abnormalities of adherent layers grown from bone marrow of patients with myelodysplasia. Br J Haematol 111:853–862.
3. Flores-Figueroa E, G Gutierrez-Espindola, JJ Montesinos, RM Arana-Trejo and H Mayani. (2002). In vitro characterization of hematopoietic microenvironment cells from patients with myelodysplastic syndrome. Leuk Res 26:687–688.
4. Wetzler M, R Kurzrock, Z Estrov, E Estey and M Talpaz. (1995). Cytokine expression in adherent layers from patients with myelodysplastic syndrome and acute myelogenous leukemia. Leuk Res 19:23–34.
5. Zhang YZ and DA WM. (2006). Expression of SDF-1 gene in bone marrow mesenchymal stem cells of patients with myelodysplastic syndrome. Zhongguo Shi Yan Xue Ye Xue Za Zhi 14:281–284.
6. Wagner W, C Roderburg, F Wein, A Diehlmann, M Frankhauser, R Schubert, V Eckstein and AD Ho. (2007). Molecular and secretory profiles of human mesenchymal stromal cells and their abilities to maintain primitive hematopoietic progenitors. Stem Cells 25:2638–2647.
7. Tauro S, MD Hepburn, Peddie CM, DT Bowen and MJ Pippard. (2002). Functional disturbance of marrow stromal microenvironment in the Myelodysplastic syndromes. Leukemia 16:785–790.
8. Wagner W, F Wein, C Roderburg, R Saffrich, A Diehlmann, V Eckstein and AD Ho. (2008). Adhesion of human hematopoietic progenitor cells to mesenchymal stromal cells involves CD44. Cells Tissues Organs 188:160–169.
9. Wagner W, F Wein, C Roderburg, R Saffrich, A Faber, U Krause, M Schubert, V Benes, V Eckstein, H Maul and AD Ho. (2007). Adhesion of hematopoietic progenitor cells to human mesenchymal stem cells as a model for cell-cell interaction. Exp Hematol 35:314–325.
10. Gottschling S, R Saffrich, A Seckinger, U Krause, K Horsch, K Miesala K and AD Ho. (2007). Human mesenchymal stromal cells regulate initial self-renewing divisions of hematopoietic progenitor cells by a beta1-integrin-dependent mechanism. Stem Cells 25:798–806.
11. Wagner W, R Saffrich, U Wirkner, V Eckstein, J Blake, A Ansorge, C Schwager, F Wein, K Miesala, W Ansorge and AD Ho. (2005). Hematopoietic progenitor cells and cellular microenvironment: behavioral and molecular changes upon interaction. Stem Cells 23:1180–1191.
12. Simmons PJ and B Torok-Storb. (1991). Identification of stromal cell precursors in human bone marrow by a novel monoclonal antibody, STRO-1. Blood 78:55–62.
13. Jones E and D McGonagle. (2008). Human bone marrow mesenchymal stem cells in vivo. Rheumatology 47:126–131.

14. Boiret N, C Rapatel, S Boisgard, S Charrier, A Tchirkov, C Bresson, L Camilleri, J Berger, L Guillouard, et al. (2003). $CD43^{+}CDw90(Thy\text{-}l)^{+}$ subset colocated with mesenchymal progenitors in human bone marrow hematon units is enriched in colony-forming unit megakaryocytes and long-term culture-initiating cells. Exp Hematol 31:1275–1283.
15. Gronthos S, E Graves, S Ohta and PJ Simmons. (1994). The $STRO\text{-}1^{+}$ fraction of adult human bone marrow contains the osteogenic precursors. Blood 84:4164–4173.
16. Psaltis PJ, S Paton, F See, A Arthur, S Martin, S Itescu, SG Worthley, S Gronthos and AC Zannettino. (2010). Enrichment for STRO-1 expression enhances the cardiovascular paracrine activity of human bone marrow-derived mesenchymal cell populations. J Cell Physiol 223:530–540.
17. Colgan SP, HK Eltzschig HK, T Eckle T and LF Thompson. (2006). Physiological roles for ecto-5′-nucleotidase (CD73). Purinergic Signal 2:351–360.
18. Airas L, J Niemelä, M Salmi, T Puurunen, DJ Smith and S Jalkanen. (1997). Differential regulation and function of CD73, a glycosyl-phosphatidylinositol–linked 70-kD adhesion molecule, on lymphocytes and endothelial cells. J Cell Biol 136:421–431.
19. Wang L, J Fan, LF Thompson, Y Zhang, T Shin, TJ Curiel and B Zhang. (2011). CD73 has distinct roles in nonhematopoietic and hematopoietic cells to promote tumor growth in mice. J Clin Investig 121:2371–2382.
20. Stochaj U and HG Mannherz. (1992). Chicken gizzard 5′-nucleotidase functions as a binding protein for the laminin/nidogen complex. Eur J Cell Biol 59:364–372.
21. Vardiman J, J Thiele, D Arber, R Brunning, M Borowitz, A Porwit, NL Harris, M Le Beau, E Hellström-Lindberg, A Tefferi and C Bloomfield. (2009). The 2008 revision of the World Health Organization (WHO) classification of myeloid neoplasms and acute leukemia: rationale and important changes. Blood 114:937–951.
22. Chevallier N, F Anagnostou, S Zilber, G Bodivit, S Maurin, A Barrault, P Bierling, P Hernigou, P Layrolle and H Rouard. (2010). Osteoblastic differentiation of human mesenchymal stem cells with platelet lysate. Biomaterials 31: 270–278.
23. Cristofalo VJ, RG Allen, RJ Pignolo, BG Martin and JC Beck. (1998). Relationship between donor age and the replicative lifespan of human cells in culture: a reevaluation. Proc Natl Acad Sci U S A 95:10614–10619.
24. Nicolaas Franken APN, HM Rodermond, J Stap, J Haveman and C van Bree. (2006). Clonogenic assay of cells in vitro. Nat Protoc 1:2315–2319.
25. Dominici M, K Le Blanc, I Mueller, I Slaper-Cortenbach, F Marini, D Krause, R Deans, A Keating, DJ Prockop and E Horwitz. (2006). Minimal criteria for defining multipotent mesenchymal stromal cells. The International Society for Cellular Therapy position statement. Cytotherapy 8:315–317.
26. Caplan AI. (2005). Review: Mesenchymal stem cells: cell–based reconstructive therapy in orthopedics. Tissue Eng 11:1198–1211.
27. Kern S, H Eichler, J Stoeve, H Klüter and K Bieback. (2006). Comparative analysis of mesenchymal stem cells from bone marrow, umbilical cord blood, or adipose tissue. Stem Cells 24:1294–1301.
28. Lee RH, MJ Seo, AA Pulin, CA Gregory, J Ylostalo and DJ Prockop. (2009). The CD34-like protein PODXL and α6-integrin (CD49f) identify early progenitor MSCs with increased clonogenicity and migration to infarcted heart in mice. Blood 113:816–826.
29. Potapova AI, PR Brink, IS Cohen and SV Doronin. (2008). Culturing of human mesenchymal stem cells as three-dimensional aggregates induces functional expression of CXCR4 That Regulates Adhesion to Endothelial Cells. J Biol Chem 283:13100–13107.
30. Prockop DJ. (2009). Repair of tissues by adult stem/progenitor cells (MSCs): controversies, myths, and changing paradigms. Am Soc Gene Ther 17:939–946.
31. Halfon S, N Abramov, B Grinblat and I Ginis. (2011). Markers distinguishing mesenchymal stem cells from fibroblasts are downregulated with passaging. Stem Cells Dev 20:53–66.
32. Short B, N Brouard, T Occhiodoro-Scott, A Ramakrishnan and PJ Simmons. (2003). Mesenchymal stem cells. Arch Med Res 35:565–571.
33. Bianco P, M Riminucci, S Gronthos and PG Robey. (2001). Bone marrow stromal cells: Nature, biology, and potential applications. Stem Cells 19:180–192.
34. Gronthos S, AC Zannettino, SJ Hay, S Shi, SE Graves, A Kortesidis and PJ Simmons. (2003). Molecular and cellular characterisation of highly purified stromal stem cells derived from human bone marrow. J Cell Sci 116:1827–1835.
35. Kohase M, D Henriksen-Destefano, LT May, J Vilček and PB Seghal. (1986). Induction of β_2-interferon by tumor necrosis factor: a homeostatic mechanism in the control of cell proliferation. Cell 45:659–666.
36. Boudard D, A Viallet, S Piselli, D Guyotat and L Campos. (2003). In vitro study of stromal cell defects in myelodysplastic syndromes. Haematologica 88:827–829.

Address correspondence to:
Dr. Carmen Mariana Aanei
Etablissement Français du Sang Bourgogne–Franche
Comté site de Nevers
1 Bd de l'Hôpital
Nevers 58000
France

E-mail: caanei@yahoo.com

Received for publication July 18, 2011
Accepted after revision September 13, 2011
Prepublished on Liebert Instant Online September 20, 2011